




Cite this: *RSC Adv.*, 2020, 10, 14235

New diterpenoid quinones derived from *Salvia miltiorrhiza* and their cytotoxic and neuroprotective activities†

Zhao-Kun Yin, Zi-Ming Feng, Jian-Shuang Jiang, Xu Zhang, Pei-Cheng Zhang * and Ya-Nan Yang *

One new tanshinone derivative, which possesses an unusual 6/6/5/6 fused-ring skeleton system (**1**), together with four new five-membered lactone benzohexa-membered ring compounds (**2**, **3**, **4A** and **4B**), and three new carboxyl substituted 5,5-spiroketal compounds (**5–7**), were isolated from the dried rhizomes of *Salvia miltiorrhiza*. The structures of these compounds were determined by multiple spectral analyses (UV, IR, NMR, and HR-ESI-MS). In addition, the absolute configurations were established by X-ray diffraction experiments, calculated and experimental circular dichroism spectra. Evaluation of antitumor activity showed that **1** had strong cytotoxicity to tumor-repopulating cells (TRCs) with an IC₅₀ value of 2.83 μM. In the evaluation of neuroprotective activity, **4A** and **6** showed a strong improvement in the survival rates of SK-N-SH cell injury induced by oxygen glucose deprivation (OGD).

Received 3rd March 2020
Accepted 20th March 2020

DOI: 10.1039/d0ra02022b

rsc.li/rsc-advances

Introduction

Diterpenoid quinones are a kind of rosin diterpenes that are mainly composed of (11,12)-*o*-phenanthraquinone and (11,14)-*p*-phenanthraquinone. The root of *Salvia miltiorrhiza* Bunge (Labiatae) is known as a traditional Chinese medicine (TCM) which was found to be abundant in diterpenoid quinones.^{1–5} Long-term pharmacological studies have found that diterpenoid quinones have significant activities, especially in terms of antitumor and cardiovascular activities.^{4–9} In recent years, with continuous deep research on this kind of component from *S. miltiorrhiza*, new derivatizations of diterpenoid quinones have been discovered. For example, two diterpenoid quinones, which have a five-membered lactone benzohexa-membered ring structure,¹⁰ and five 5,5-spiroketal,^{12–14} have been isolated from *S. miltiorrhiza* Bunge (Labiatae), with these two components having neoteric basic skeleton forms of 6/6/5, 6/6/5/5 respectively. Although the amount of each compound was less, the discovery of these compounds with novel structures and significant activities reinvigorated our enthusiasm for the in-depth exploration of *S. miltiorrhiza*.

In a study of the biologically active constituents in the ethyl acetate-soluble portion of *S. miltiorrhiza* root bark, which was

acquired from an 80% EtOH extract, one new tanshinone derivative (**1**), which possessed an unusual ring-C compared with the common tanshinone skeleton, was obtained (Fig. 1). Furthermore, four new diterpenoid quinones (**2**, **3**, **4A** and **4B**), which all contained a 6/6/5 skeleton, and three new 5,5-spiroketal compounds (**5–7**) that had the feature of a carboxylic acid-substituted helical lactone ring, were isolated. Based on the source route analysis, these three types of components were all derived from (11,12)-*o*-phenanthraquinone or (11,14)-*p*-phenanthraquinone. Evaluation of antitumor activity and neuroprotective activity results of these isolated products were also reported.

Results and discussion

Compound **1** was isolated as white amorphous powder. Its molecular formula was established as C₁₈H₁₆O₅ by its negative HRESIMS ion at *m/z* 311.0924 [M – H][–] (calcd for C₁₈H₁₅O₅, 311.0925), which indicated 11 degrees of unsaturation. The IR spectrum showed the absorptions of hydroxy (3433 cm^{–1}), carbonyl (1725 cm^{–1}) and olefinic (1616 cm^{–1}) groups. Its ¹H NMR data (Table 1) were indicative of an AMX pattern for three aromatic protons at δ_H 8.32 (1H, d, *J* = 8.5 Hz, H-1), 7.65 (1H, dd, *J* = 6.5, 8.5 Hz, H-2), and 7.61 (1H, d, *J* = 6.5 Hz, H-3) and a pair of *ortho*-aromatic protons at δ_H 8.30 (1H, d, *J* = 8.5 Hz, H-6), 7.79 (1H, d, *J* = 8.5 Hz, H-7). This information, together with a methyl signal at δ_H 2.72 (3H, s, H-18), indicated that **1** contained a 4-methylnaphthalene unit, which was similar to that of tanshinone I.¹⁹ In addition, two oxygenated methylene protons at δ_H 3.95 (1H, dd, *J* = 3.5, 12.0 Hz, H-15a), 3.15 (1H, t, *J* = 12.0 Hz, H-15b), one methine proton at δ_H 2.28 (1H, m, H-16),

State Key Laboratory of Bioactive Substance and Function of Natural Medicines, Peking Union Medical College, Institute of Materia Medica, Chinese Academy of Medical Sciences, Beijing 100050, China. E-mail: pczhang@imm.ac.cn; yyn@imm.ac.cn; Fax: +86 10 63017757; Tel: +86 10 63165231

† Electronic supplementary information (ESI) available. CCDC 1975214. For ESI and crystallographic data in CIF or other electronic format see DOI: 10.1039/d0ra02022b



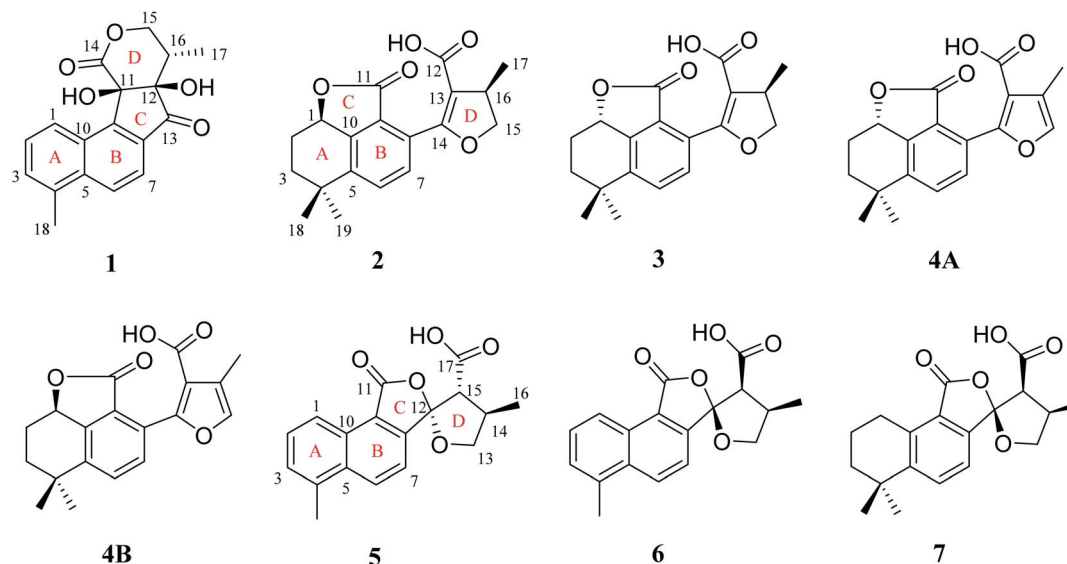


Fig. 1 The structures of compounds 1–7.

and one methyl signal at δ_{H} 0.93 (3H, d, $J = 7.5$ Hz, H-17), were observed in the upfield region of the ^1H NMR spectrum. The ^{13}C NMR data (Table 1) and HSQC spectra revealed 18 carbon signals; apart from 11 carbons assigned to the 4-methylnaphthalene unit, the remaining seven carbons could be attributed to four quaternary carbons, one methine carbon, one methylene carbon and one methyl group. In the HMBC spectrum, the correlations from H-15 to C-12, C-16, and C-17, H-16 to C-12, C-

13, C-15, and C-17, as well as OH-12 to C-12, C-13, and C-16 revealed the presence of a 2,4-dihydroxy-3-methyl butanone moiety in 1 (Fig. 2). Additionally, the characteristic HMBC correlations from H-15 to C-14, H-7 to C-13, OH-11 to C-11, C-9, and C-12 established the unusual five-membered ring (ring C) and six-membered ring (ring D) in 1, which consisted of C-8/C-9/C-11/C-12/C-13 and C-11/C-12/C-14/O/C-15/C-16. Then, the

Table 1 ^1H NMR (500 MHz) and ^{13}C NMR (125 MHz) data of compounds 1–4

No.	1 ^a		2 ^b		3 ^b		4A/4B ^b	
	δ_{H} (J in Hz)	δ_{C}	δ_{H} (J in Hz)	δ_{C}	δ_{H} (J in Hz)	δ_{C}	δ_{H} (J in Hz)	δ_{C}
1	8.32, d (8.5)	123.2	5.19, dd (5.5, 12.0)	78.0	5.19, dd (5.5, 12.0)	77.8	5.22, dd (5.5, 11.5)	77.8
2	7.65, dd (6.5, 8.5)	127.8	2.39, m, 1.62, m, 1.62, m	26.3	2.39, m, 1.62, m	26.3	2.40, m, 1.62, m	26.3
3	7.61, d (6.5)	130.5	1.92, m, 1.85, m	38.0	1.92, m, 1.85, m	38.2	1.92, m, 1.86, m	37.1
4		133.5		34.9		34.9		34.9
5		135.9		144.6		144.8		144.1
6	8.30, d (8.5)	128.4	7.55, d (8.0)	131.1	7.55, d (8.0)	131.5	7.65, d (8.0)	131.2
7	7.79, d (8.5)	118.3	7.47, d (8.0)	130.0	7.47, d (8.0)	130.0	7.52, d (8.0)	130.3
8		129.2		126.9		126.8		126.5
9		148.9		122.9		123.2		123.0
10		136.4		148.0		148.0		148.3
11		78.9		168.5		168.5		168.9
12		83.4		170.1		170.1		169.0
13		202.0		111.5		111.6		122.5
14		173.0		163.3		163.0		154.0
15	3.95, dd (3.5, 12.0), 3.15, t (12.0)	68.2	4.72, t, (9.0), 4.23, dd (5.5, 9.0)	78.9	4.70, t (9.0), 4.24, dd (5.5, 9.0)	78.9	7.32, s	140.6
16	2.28, m	40.5	3.49, m	37.2	3.40, m	37.1		117.0
17	0.93, d (7.5)	11.3	1.34, d (6.5)	19.6	1.38, d, (7.0)	20.0	2.23, s	10.1
18	2.72, s	19.6	1.44, s	31.8	1.44, s	31.8	1.45, s	31.8
19			1.19, s	30.9	1.19, s	31.0	1.22, s	31.0
OH-11	6.70, s							
OH-12	6.34, s							

^a Data were measured in DMSO- d_6 . ^b Data were measured in CDCl_3 .



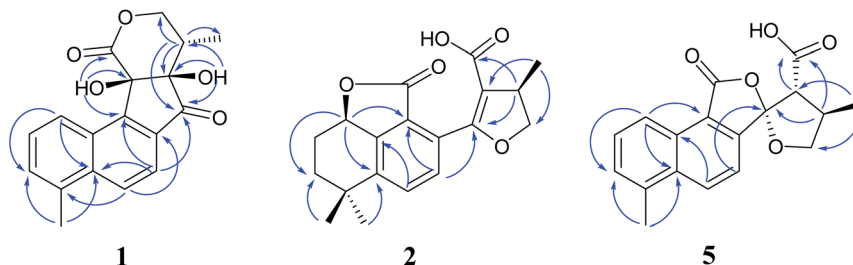


Fig. 2 Key HMBC correlations of compounds 1, 2, 5.

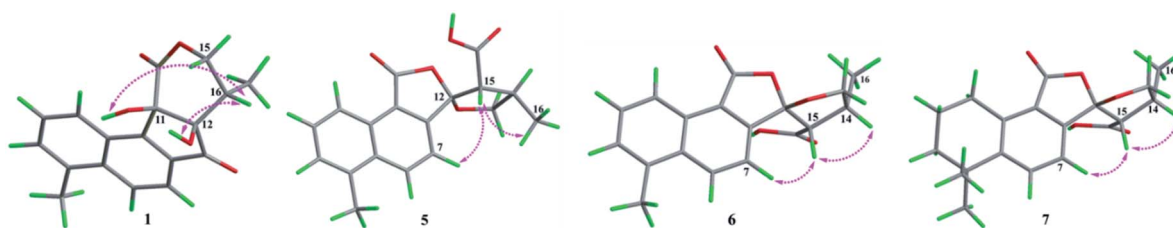


Fig. 3 The ROESY correlations of compounds 1, 5–7.

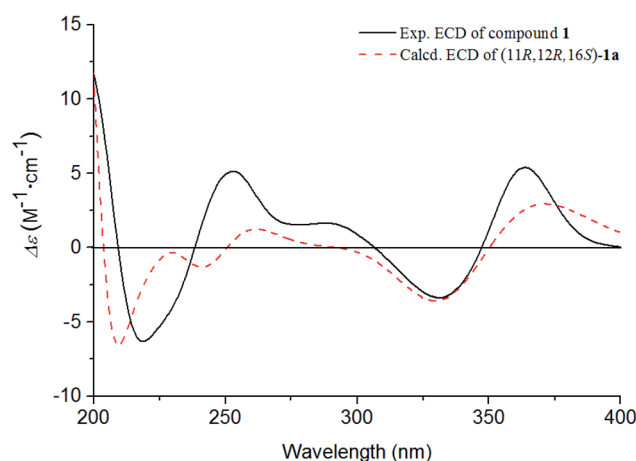
planar structure was elucidated as shown in Fig. 1 with a 6/6/5/6-membered ring skeleton.

The absolute configurations of C-11, C-12, and C-16 were identified by the ROESY experiment and comparison of the experimental and calculated ECD spectra. In the ROESY experiment, the correlations from OH-11 to H-16 and OH-12 confirmed the *cis*-relationship between OH-11 and H-16, as well as the *cis*-relationship between OH-11 and OH-12 (Fig. 3). This result was further verified by a strong correlation from OH-12 to H-16, together with a weak correlation from OH-12 to H-17. From the above analysis, **1** had only one pair of enantiomers (**1a**: 11*R*,12*R*,16*S* and **1b**: 11*S*,12*S*,16*R*). A systematic conformational analysis was performed for **1a** using a molecular mechanics force field (MMFF94) calculation. The optimized conformation of **1a** was further obtained using the time-dependent density functional theory (TDDFT) method at the B3LYP/6-311+G (d, p) level. The overall calculated ECD spectra of **1a** was established based on the Boltzmann weighting of the lowest energy conformers. Finally, the calculated ECD spectrum of **1a** was matched with the experimental result over the entire range of wavelengths (Fig. 4). Based on the above evidence, the structure of **1** was determined to be as shown in Fig. 1 and was named tanshin cyclopentanone A.

Compound **2**, obtained as white massive crystal, was indicated to have the molecular formula of $C_{19}H_{20}O_5$ according to the HRESIMS m/z 351.1198 $[M + Na]^+$ (calcd for $C_{19}H_{20}NaO_5$, 351.1203). The IR spectrum indicated that **2** contained carboxyl (2955, 1766 cm^{-1}) and carbonyl (1666 cm^{-1}) functional groups. Its ^{13}C NMR data (Table 1) showed 19 carbon signals, including two carbonyl carbons, eight aromatic carbon signals and nine aliphatic carbon signals. In the 1H NMR data (Table 1), a group of aromatic hydrogen signals appeared in the downfield region at δ_H 7.55 (1H, d, $J = 8.0$ Hz, H-6), 7.47 (1H, d, $J = 8.0$ Hz, H-7). A set of $-CH_2CH_2-$ characteristic signals were observed at δ_H 2.39

(1H, m, H-2a), 1.62 (2H, m, H-2b), 1.92 (1H, m, H-3a), 1.85 (1H, m, H-3b). In the upfield region, based on the HSQC spectrum, the characteristic signals of a methyl substituted dihydrofuran ring at δ_H 4.72 (1H, t, $J = 9.0$ Hz, H-15a), 4.23 (1H, dd, $J = 5.5$, 9.0 Hz, H-15b), 3.49 (1H, m, H-16), 1.34 (3H, d, $J = 6.5$ Hz, H-17) were observed. The 1D NMR information of **2** was almost identical to the 1*R*-hydroxy-anhydride of 16*R*-cryptotanshinone,¹⁵ which was obtained *via* biotransformation by *Mucor rouxii*. Moreover, the HMBC correlations found in **2** were also the same as those of the 1*R*-hydroxy-anhydride of 16*R*-cryptotanshinone (Fig. 2).

However, the single-crystal X-ray diffraction experiment (Cu $K\alpha$ radiation) showed that **2** possessed a 6/6/5 skeleton structure rather than a 6/6/7/5 skeleton of 1*R*-hydroxy-anhydride of 16*R*-cryptotanshinone (Fig. 5). This result showed that it is difficult to distinguish **2** and 1*R*-hydroxy-anhydride of 16*R*-cryptotanshinone

Fig. 4 Experimental and calculated ECD spectra of **1**.

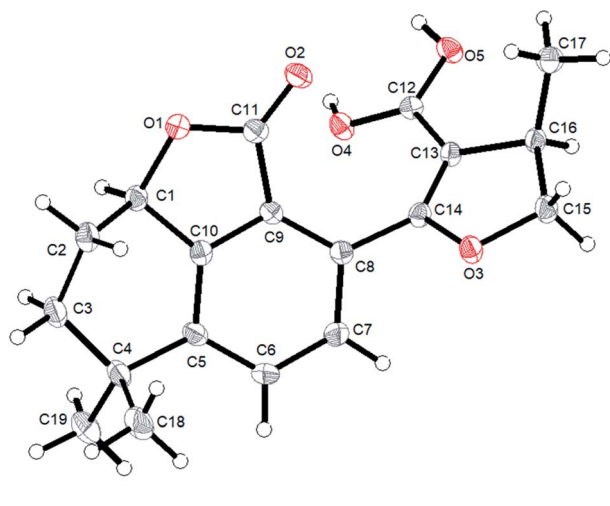


Fig. 5 ORTEP diagram of 2.

only by using the 2D NMR data. The absolute configurations of **2** were determined to be *1R,16R* according to the X-ray diffraction analysis. This result was also confirmed by the calculated ECD data of (*1R,16R*)-**2**, which matched well with the experimental ECD data of **2** (Fig. S8, ESI†). Therefore, the structure of **2** was established and named salvianolactone acid A.

Compound **3** was isolated as white amorphous powder, and had the same molecular formula as **2** based on the HRESIMS m/z 351.1198 $[M + Na]^+$ (calcd for $C_{19}H_{20}NaO_5$, 351.1203). The UV spectrum and 1D, 2D NMR data of **3** were also similar to **2**, and these features illustrated that **3** possessed the same planar construction with **2**. However, the HPLC analysis and the nuances of the 1D NMR data between **2** and **3** indicated that **3**

not an enantiomer but an epimer of **2**. The absolute configurations of **3** might be **3a** (*1S,16R*) or **3b** (*1R,16S*). As a result of the experimental and calculated ECD spectra, the calculated ECD data of **3a** matched well with the experimental ECD data of **3** (Fig. S9, ESI†). Thus, the structure of **3** was determined and named salvianolactone acid B.

Compounds **4A** and **4B** are a pair of enantiomers, which were obtained through chiral *pre*-HPLC. Their molecular formulas were determined to be $C_{19}H_{18}O_5$ based on the HRESIMS m/z 325.1079 $[M - H]^-$ (calcd for $C_{19}H_{17}O_5$, 325.1082). Analysis of the 1D NMR data of **3** and **4A/4B** revealed that the main difference between **3** and **4A/4B** was ring D. The chemical shifts of C-15 (δ_C 140.6) and C-16 (δ_C 117.0) confirmed the furan ring moiety in **4A/4B**, which was supported by the HMBC correlations of CH₃-17 with C-13, C-15, C-16, H-7 with C-5, C-9, C-14, and H-15 with C-13, C-14, C-16.

The absolute configurations of this pair of enantiomers were established by experimental and calculated ECD. As a result, the (*1S*)-enantiomer matched well with the experimental ECD spectra of **4A**, and the (*1R*)-enantiomer was in agreement with the experimental ECD spectra of **4B** (Fig. S10, ESI†). Therefore, the structures of **4A** and **4B** were elucidated and named salvianolactone acid C and salvianolactone acid D, respectively.

Compound **5**, a white amorphous powder, had the molecular formula of $C_{18}H_{16}O_5$ as established by the HRESIMS ion at m/z 311.0927 $[M - H]^-$ (calcd for $C_{18}H_{15}O_5$, 311.0925). The IR spectrum indicated that **5** contained carbonyl groups (1762 and 1726 cm^{-1}). The 1H NMR data (Table 2) of **5** was showed to have the typical structure of the methyl substituted naphthalene ring and included an AMX pattern at δ_H 8.78 (1H, d, $J = 8.5$ Hz, H-1), 7.56 (1H, dd, $J = 7.0, 8.5$ Hz, H-2), 7.44 (1H, d, $J = 7.0$ Hz, H-3), a group of *ortho*-aryl hydrogen signals at δ_H 8.33 (1H, d, $J = 8.5$ Hz, H-6), 7.55 (1H, d, $J = 8.5$ Hz, H-7), and one methyl group

Table 2 1H NMR (500 MHz) and ^{13}C NMR (125 MHz) data of compounds 5–7 in $CDCl_3$

No.	5		6		7	
	δ_H (J in Hz)	δ_C	δ_H (J in Hz)	δ_C	δ_H (J in Hz)	δ_C
1	8.78, d (8.5)	122.5	8.82, d (8.5)	122.4	3.17, t (6.0)	26.1
2	7.56, dd (7.0, 8.5)	129.1	7.57, t (7.0, 8.5)	129.1	1.82, m	18.6
3	7.44, d (7.0)	128.7	7.45, d (7.0)	128.7	1.68, m	38.4
4		129.3		129.3		34.6
5		133.7		133.7		149.2
6	8.33, d (8.5)	132.3	8.32, d (8.5)	132.1	7.62, d (8.0)	133.2
7	7.55, d (8.5)	118.0	7.48, d (8.5)	117.7	7.18, d (8.0)	118.9
8		146.2		146.4		144.4
9		122.2		122.9		124.5
10		135.3		135.2		137.9
11		168.2		168.5		169.0
12		111.4		109.8		109.8
13	4.51, t (8.0), 3.85, t (8.0)	76.1	4.45, t (8.0), 4.07, dd (3.5, 8.5)	76.6	4.36 t (7.5), 3.97, dd (3.5, 8.5)	76.2
14	3.22, m	34.6	3.04, m	34.4	2.94, m	34.3
15	3.20, overlap	59.2	3.63, d (8.0)	54.7	3.48, d (8.0)	55.4
16	1.32, d (5.5)	17.1	1.43, d (7.0)	16.3	1.28, s	16.1
17		172.2		171.6		172.3
18	2.71, s	20.0	2.72, s	20.0	1.30, s	32.0
19					1.30, s	31.9



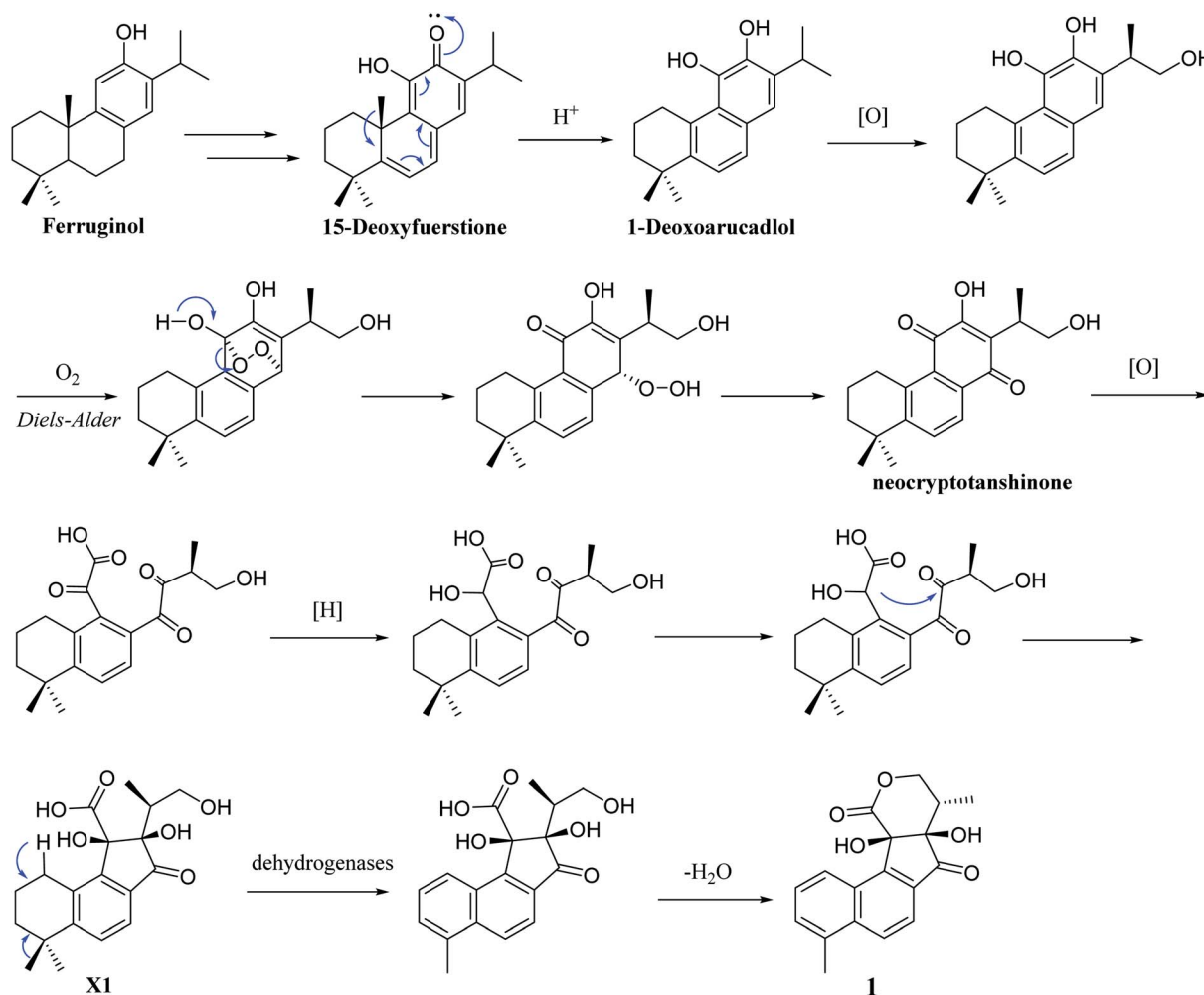
at δ_{H} 2.71 (3H, s, H-18). The ^{13}C NMR data (Table 2) displayed 18 carbon signals; in addition to the 11 carbon signals on the methyl substituted naphthalene ring unit, **5** contained two carbonyl groups (δ_{C} 168.2, 172.2), one oxygenated quaternary carbon group (δ_{C} 111.4), two methine groups (δ_{C} 34.6, 59.2), one methylene group (δ_{C} 76.1) and one methyl group (δ_{C} 17.1). These NMR data were similar to those of *epi*-danshenspiroketallactone A,¹² except for the ethyl ester group in *epi*-danshenspiroketallactone A. The HMBC correlations (Fig. 2) of H-7 with C-5, C-9, C-12, CH₃-16 with C-13, C-14, C-15, H-14 with C-17, and CH₃-16 with C-17 were verified the planar structure of **5** as shown in Fig. 1.

In the case of CDCl₃ as a deuterated reagent, H-13 and H-16 overlapped. Therefore, DMSO-*d*₆ was used as the deuterated reagent, and these two signals can be separated and appeared at δ_{H} 3.59 (1H, d, *J* = 11.0 Hz, H-13) and 2.95 (1H, m, H-16), respectively (Table S1, ESI†). In the NOE spectrum (Fig. S56, ESI†), irradiation of CH₃-16 enhanced H-15. Furthermore, the ROESY correlations (Fig. 3) of H-7 with H-15, H-15 with CH₃-16 indicated that the absolute configurations of **5** might be **5a** (12*S*,14*R*,16*R*) or **5b** (12*R*,14*S*,16*S*). The calculated ECD spectra of **5a** and **5b** showed that **5a** agreed with the experimental

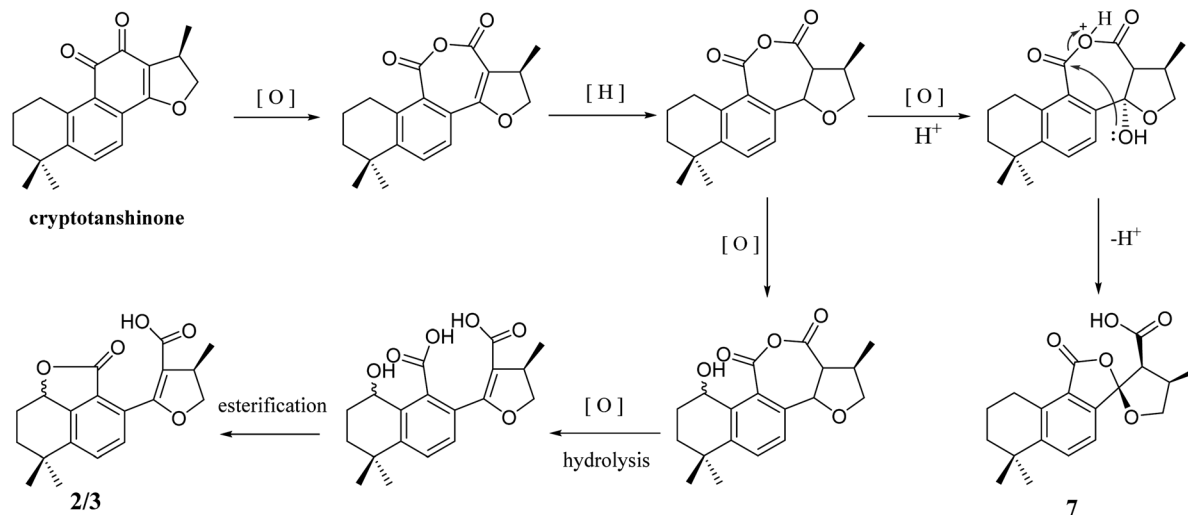
spectrum of **5** (Fig. S11, ESI†); therefore, the structure of **5** was determined and named *epi*-danshenspiroketallactone B.

The planar structure of **6** was established as the same as **5** based on the 1D and 2D NMR data. The NOE spectrum (Fig. S67, ESI†) showed that irradiation with H-14 enhanced H-15. What's more, the ROESY experiment displayed that H-14 had correlation with H-15, and H-7 had correlation with H-15 (Fig. 3). Therefore, the absolute configurations of **6** might be **6a** (12*R*,14*R*,15*S*) or **6b** (12*S*,14*S*,15*R*). In the calculated ECD results, the spectrum of **6a** agreed with the experimental spectrum of **6** (Fig. S12, ESI†), so the structure of **6** was established and named *epi*-danshenspiroketallactone C.

Compound **7** was isolated as white amorphous powder and had the molecular formula of C₁₉H₂₂O₅ via the HRESIMS ion at *m/z* 329.1396 [M – H][–] (calcd for C₁₉H₂₁O₅, 329.1395). The ^1H NMR data (Table 2) showed two aromatic protons, four methylene groups, two methine groups and three methyl groups. The ^{13}C NMR spectrum (Table 2) of **7** displayed 19 carbon signals. Comparison of **7** with **6** showed that the main difference was in the structure of ring A. The chemical shifts of δ_{H} 3.17 (2H, t, *J* = 6.0 Hz, H-1), 1.82 (2H, m, H-2), 1.68 (2H, m, H-3) and δ_{H} 1.30 (6H, s, H-18,19) confirmed the dimethyl substituted six-



Scheme 1 Plausible biogenetic pathway for **1**.



Scheme 2 Plausible biogenetic pathway for 2/3 and 7.

membered ring of 7, which was also determined by the HMBC correlations of H-1 with C-2, C-3, C-5, C-9, C-10 and H-18/19 with C-3, C-4, and C-5.

In the NOE spectrum (Fig. S78, ESI[†]), irradiation of H-14 enhanced H-15. What's more, the ROESY correlations (Fig. 3) of H-15 with H-14, H-7 with H-15 illustrated that the absolute configurations of 7 might be either **7a** (12*R*,14*R*,16*S*) or **7b** (12*S*,14*S*,16*R*). Both **7a** and **7b** underwent ECD calculations, and **7a** matched the experimental spectrum of 7 (Fig. S13, ESI[†]), so the structure of 7 was finally determined and named *epi*-danthenspiroketalactone D.

Structurally, **1** represents a new skeleton of tanshinone derivative with an unusual 6/6/5/6-membered ring skeleton. Its distinctive biogenetic route is proposed in Scheme 1. A literature survey indicated that the essential precursor neocryptotanshinone,¹⁶ which was isolated from the roots of *S. miltiorrhiza* previously, might be derived from ferruginol through a series of aromatization, oxidation, Diels-Alder reaction, rearrangement, hydrogenation and oxidation reactions. Subsequently, neocryptotanshinone formed **XI** through the oxidative cracking of ring C, hydrogenation, and cyclization. Finally, **1** was formed by aromatization and lactonization of **XI**. In particular, during the procedure of forming of **1**, the key process is the construction of a cyclopentanone moiety, which is unique in the tanshinone derivative. According to the above biosynthetic pathway perspective, the absolute configuration of C-16 remained constant during the progression of ring cracking and recycling of neocryptotanshinone.^{17,18}

In addition, 2–7 contained two types of skeleton structures, which might all derive from cryptotanshinone (Scheme 2).¹¹ During a series of oxidation, hydrogenation, and cracking rearrangement of ring C/D under active enzymatic steps, cryptotanshinone could derive various products with multiple structures.¹⁰

TRCs play an important role during the process of tumor migration and recurrence. Therefore, it is a research hotspot to explore an effective targeted agent to kill TRCs. An *in vitro* assay

showed that **1** had strong cytotoxicity toward A375 TRCs (IC₅₀ = 2.83 μM), which were generated from a 3D fibrin gel culture system.²⁰ Delightedly, **1** exhibited no cytotoxicity to the nonstem-like A375 cancer cells at a concentration of 100 μM by the MTT method. This result implied that **1** might be a potent targeted antitumor agent with less adverse effects. In the evaluation of neuroprotective activities, **4A** showed obvious activity to increase the survival rate (13.08%) of SK-N-SH cell injury induced by oxygen glucose deprivation (OGD) compared with the positive control drug PHPB (7.43%). And under the same activity screening model, compound **6** also showed a noteworthy improvement in the survival rate (10.48%) compared with PHPB.

Experimental

General experimental procedures

The optical rotations and ECD spectra were experimented by RUDOLPH automatic V polarimeter JASCO V650 and J-815 spectrometer (JASCO, Easton, MD, USA), respectively. The UV spectra was measured on JASCO V-650. The IR data were measured on Nicolet 5700 spectrometer (Thermo Scientific, FL, USA). The NMR spectra were recorded with Bruker 500 MHz (Bruker-Biospin, Billerica, MA, USA) and 600 MHz NMR spectrometers (Varian, Inc., Palo Alto, CA, USA). HRESIMS reports were obtained from Agilent 6520 HPLC-Q-TOF (Agilent Technologies, Waldbronn, Germany). Preparative HPLC was performed using a Shimadzu LC-10AT with an ODS-A column (250 mm × 20 mm, 5 μm; YMC Corp., Kyoto, Japan). The Agilent 1260 series system coupled with an Apollo C18 column (250 mm × 4.6 mm, 5 μm; Alltech Corp., KY, USA) were used for HPLC-DAD experiments. RP-18 (50 μm, YMC Corp., Kyoto, Japan), Sephadex LH-20 (Pharmacia Fine Chemicals, Uppsala, Sweden), and silica gel (200–300 mesh, Qingdao Ocean Chemical Plant) were used as chromatographic substrates. Chiral-phase separation was performed by the Chiralpak AD-RH and AD-H chiral column (250 mm × 10 mm, 5 μm; Daicel Corp., Tokyo, Japan). Analytical chiral-phase HPLC was performed by



the Chiralpak AD-RH chiral column (250 mm × 4.6 mm, 5 μm; Daicel Corp., Tokyo, Japan).

Fungal material

The dried rhizomes of *Salvia miltiorrhiza* were collected in Rizhao City (Shandong Province, China) in March 2017; the plant was authenticated by Lin Ma. A voucher specimen (herbarium no. ID-S-2944) has been deposited at the herbarium of the Department of Medicinal Plants, Institute of Materia Medica, Chinese Academy of Medical Sciences, Beijing, China.

Extraction and isolation

The dried rhizomes of *Salvia miltiorrhiza* (70 kg) were smashed and extracted with 80% EtOH (3 × 100 L) at 85 °C for 2 h. The extract was concentrated under reduced pressure to obtained 23 kg of paste. Add water in the paste to make a suspension and extract four times with ethyl acetate. The ethyl acetate extract (2.2 kg) was subjected to silica gel (200–300 mesh) open column chromatography with a stepwise gradient of petroleum ether–acetone (100/0 to 0/100) gave twelve fractions (Fr.1–12). Fr.6 and Fr.7 (a total of about 100 g) were further subjected to column chromatography over silica gel and eluted with a gradient of PE–EtOAc to yield fractions y1–y30. Then, Fr.y22–Fr.y24 (27.6 g) was separated by silica gel column chromatography eluted with a gradient of PE–EtOAc mobile phase system and finally give six fractions A–F (2.38, 3.15, 5.87, 6.66, 6.89 and 1.80 g, respectively). Fraction E was further separated by Sephadex LH-20 (CH₂Cl₂–MeOH, gradient) and RP-HPLC (MeOH–H₂O = 70 : 30 for first time; MeCN–H₂O = 50 : 50 for second time) to yield compound 2 (82.6 mg), compound 3 (27.3 mg), compound 4A/4B (21.5 mg). Fr.y25–Fr.y29 (16.8 g) was separated by silica gel column chromatography eluted with a gradient of dichloromethane–methanol mobile phase system to yield five fractions A1–E1 (4.85, 3.16, 2.65, 3.22 and 2.53 g, respectively). Fraction D1 were further separated by Sephadex LH-20 (CH₂Cl₂–MeOH, gradient) and RP-HPLC (MeOH–H₂O = 70 : 30 for first time; MeCN–H₂O = 50 : 50 for second time) to yield compound 1 (4.9 mg), compound 5 (10.2 mg), compound 6 (21.0 mg), compound 7 (7.0 mg). The flow rate of the RP-HPLC was 1 mL min^{−1}, and the detection wavelength was 254 nm.

Tanshin cyclopentanone A (1). White, amorphous powder; $[\alpha]_D^{20} +173$ (c 0.1, MeOH); UV (MeOH) λ_{\max} (log ϵ) 210 (2.10), 257 (2.51), 293 (1.69), 349 (1.22) nm; IR ν_{\max} 3433, 2958, 2929, 1725, 1616, 1593, 1469, 1383, 1246, 1125, 1022, 822, 779 cm^{−1}; CD (MeOH) 219 ($\Delta\epsilon$ −6.30), 253 ($\Delta\epsilon$ +5.13), 331 ($\Delta\epsilon$ −3.37), 364 ($\Delta\epsilon$ +5.38) nm; ¹H NMR (DMSO-*d*₆, 500 MHz) and ¹³C NMR (DMSO-*d*₆, 125 MHz) spectroscopic data, see Table 1; HR-ESI-MS m/z 311.0924 [M − H][−] (calcd for C₁₈H₁₅O₅, 311.0925).

Salvianolactone acid A (2). White, massive crystal, $[\alpha]_D^{20} -193.4$ (c 0.1, MeOH); UV (MeOH) λ_{\max} (log ϵ) 210 (2.39), 241 (2.01), 308 (1.61) nm; IR ν_{\max} 2955, 2649, 1766, 1666, 1493, 1338, 1247, 1072, 1007, 945, 844 cm^{−1}; CD (MeOH) 215 ($\Delta\epsilon$ +3.59), 234 ($\Delta\epsilon$ −0.78), 260 ($\Delta\epsilon$ +4.30), 322 ($\Delta\epsilon$ −3.05); ¹H NMR (CDCl₃, 500 MHz) and ¹³C NMR (CDCl₃, 125 MHz) spectroscopic data, see Table 1; HR-ESI-MS m/z 351.1198 [M + Na]⁺ (calcd for C₁₉H₂₀NaO₅, 351.1203).

Salvianolactone acid B (3). White, amorphous powder, $[\alpha]_D^{20} +154$ (c 0.1, MeOH); UV (MeOH) λ_{\max} (log ϵ) 210 (2.36), 240 (2.00), 304 (1.58) nm; IR ν_{\max} 2961, 2871, 1767, 1664, 1497, 1440, 1072, 1045, 1005, 945, 843 cm^{−1}; CD (MeOH) 231 ($\Delta\epsilon$ +1.47), 257 ($\Delta\epsilon$ −1.68), 296 ($\Delta\epsilon$ +1.18) nm; ¹H NMR (CDCl₃, 500 MHz) spectroscopic data and ¹³C NMR (CDCl₃, 125 MHz), see Table 1; HR-ESI-MS m/z 351.1198 [M + Na]⁺ (calcd for C₁₉H₂₀NaO₅, 351.1203).

Salvianolactone acid C/D (4A/4B). White, amorphous powder, $[\alpha]_D^{20} +263$ (c 0.1, MeOH) (4A), $[\alpha]_D^{20} -188$ (c 0.1, MeOH) (4B); UV (MeOH) λ_{\max} (log ϵ) 207 (2.41), 241 (2.07), 295 (1.74), 329 (1.91) nm; IR ν_{\max} 2961, 2868, 1766, 1687, 1554, 1490, 1435, 1301, 1219, 1069, 1005, 970, 841 cm^{−1}; CD (MeOH) 240 ($\Delta\epsilon$ +2.16), 262 ($\Delta\epsilon$ −6.09), 325 ($\Delta\epsilon$ +3.01) nm (4A), CD (MeOH) 239 ($\Delta\epsilon$ −3.89), 261 ($\Delta\epsilon$ +4.50), 325 ($\Delta\epsilon$ −2.32) nm (4B); ¹H NMR (DMSO-*d*₆, 500 MHz) spectroscopic data and ¹³C NMR (CDCl₃, 125 MHz), see Table 1; HR-ESI-MS m/z 325.1079 [M − H][−] (calcd for C₁₉H₁₇O₅, 325.1082).

epi-Danshenspiroketallactone B (5). White, amorphous powder, $[\alpha]_D^{20} +39$ (c 0.1, MeOH); UV (MeOH) λ_{\max} (log ϵ) 211 (2.44), 244 (2.39), 313 (1.65) nm; IR ν_{\max} 3567, 2894, 1762, 1726, 1587, 1329, 1305, 1242, 1206, 1071, 985, 818 cm^{−1}; CD (MeOH) 239 ($\Delta\epsilon$ −7.52), 260 ($\Delta\epsilon$ +4.13) nm; ¹H NMR (CDCl₃, 500 MHz) and ¹³C NMR (CDCl₃, 125 MHz) spectroscopic data, see Table 2, ¹H NMR (DMSO-*d*₆, 500 MHz) spectroscopic data, see Table S1 in ESI;† HR-ESI-MS m/z 311.0927 [M − H][−] (calcd for C₁₈H₁₅O₅, 311.0925).

epi-Danshenspiroketallactone C (6). White, amorphous powder, $[\alpha]_D^{20} -38$ (c 0.1, MeOH); UV (MeOH) λ_{\max} (log ϵ) 211 (2.37), 244 (2.33), 313 (1.59) nm; IR ν_{\max} 3567, 3449, 2977, 1750, 1717, 1586, 1335, 1192, 1060, 974, 815 cm^{−1}; CD (MeOH) 207 ($\Delta\epsilon$ +1.90), 222 ($\Delta\epsilon$ −0.94), 240 ($\Delta\epsilon$ +3.86), 259 ($\Delta\epsilon$ −2.75), 304 ($\Delta\epsilon$ −0.93), 326 ($\Delta\epsilon$ −0.76) nm; ¹H NMR (CDCl₃, 500 MHz) and ¹³C NMR (CDCl₃, 125 MHz) spectroscopic data, see Table 2, ¹H NMR (DMSO-*d*₆, 500 MHz) spectroscopic data, see Table S1 in ESI;† HR-ESI-MS m/z 311.0927 [M − H][−] (calcd for C₁₈H₁₅O₅, 311.0925).

epi-Danshenspiroketallactone D (7). White, amorphous powder, $[\alpha]_D^{20} +4$ (c 0.1, MeOH); UV (MeOH) λ_{\max} (log ϵ) 208 (2.44), 241 (1.63), 291 (1.18) nm; IR ν_{\max} 3209, 2959, 1757, 1594, 1432, 1335, 1308, 1175, 1061, 927, 832 cm^{−1}; CD (MeOH) 217 ($\Delta\epsilon$ +1.50), 253 ($\Delta\epsilon$ −1.25) nm; ¹H NMR (CDCl₃, 500 MHz) and ¹³C NMR (CDCl₃, 125 MHz) spectroscopic data, see Table 2, ¹H NMR (DMSO-*d*₆, 500 MHz) spectroscopic data, see Table S1 in ESI;† HR-ESI-MS m/z 329.1396 [M − H][−] (calcd for C₁₉H₂₁O₅, 329.1395).

X-ray crystallographic data for salvianolactone acid A

Salvianolactone acid A (2) was recrystallized from CH₂Cl₂ and MeOH (3 : 1) to give colorless block crystals. The X-ray crystallographic structure of 2 was obtained by anomalous scattering of Cu K α radiation. Crystal data: C₁₉H₂₀O₅, $M = 328.35$, hexagonal, $a = 14.63788(16)$ Å, $c = 13.6616(2)$ Å, $U = 2535.06(7)$ Å³, $T = 109.90(10)$, space group $P6_4$ (no. 172), $Z = 6$, $\mu(\text{Cu K}\alpha) = 0.767$, 14 929 reflections measured, 3057 unique ($R_{\text{int}} = 0.0262$) which were used in all calculations. The final $wR(F_2)$ was 0.0771 (all data). Flack parameter, $x = 0.09(6)$. The complete data were

deposited at the Cambridge Crystallographic Data Centre (CCDC 1975214).†

Antitumor activities of compounds 1–7

The details evaluation method of antitumor activities is same as involved in the literature.²⁰

Neuroprotective activities of compounds 1–7

The screening method of neuroprotective activities refer to the literature.²¹

Conclusion

A tanshinone derivative (**1**) with an unusual 6/6/5/6 skeleton structure, four new diterpenoid quinones (**2**, **3**, **4A** and **4B**), and three new 5,5-spiroketal compounds (**5**–**7**) were isolated from the roots of *Salvia miltiorrhiza*. All of the compounds were screened for their antitumor and neuroprotective activities. The results indicated that **1** had strong cytotoxicity to A375 TRCs (IC₅₀ = 2.83 μM); **4A** and **6** showed obvious neuroprotective activities based on the increased survival rate of SK-N-SH cell injury induced by oxygen glucose deprivation (OGD).

Conflicts of interest

The authors have no conflicts of interest to declare.

Acknowledgements

This research was financially supported by Fundamental Research Funds for CAMS/PUMC (2018RC350011), The Drug Innovation Major Project (2018ZX09711001-008), and the Chinese Academy of Medical Sciences (CAMS) Innovation Fund for Medical Sciences (No. 2017-I2M-3-010).

References

- M. H. Li, Q. Q. Li, C. H. Zhang, N. Zhang, Z. H. Cui, L. Q. Huang and P. G. Xiao, *Acta Pharm. Sin. B*, 2013, **3**, 273–280.
- G. H. Du and J. T. Zhang, *Her. Med.*, 2004, **23**, 355–360.
- J. J. Wu, Q. L. Ming, X. Zhai, S. Q. Wang, B. Zhu, Q. L. Zhang, Y. B. Xu, S. S. Shi, S. C. Wang, Q. Y. Zhang, T. Han and L. P. Qin, *Carbohydr. Polym.*, 2019, **223**, 115125.
- C. Y. Su, Q. L. Ming, K. Rahman, T. Han and L. P. Qin, *Chin. J. Nat. Med.*, 2015, **13**, 163–182.
- Y. B. Wu, Z. Y. Ni, Q. W. Shi, M. Dong, H. Kiyota, Y. C. Gu and B. Cong, *Chem. Rev.*, 2012, **112**, 5967–6026.
- A. Watzke, S. J. O'Malley, R. G. Bergman and J. A. Ellman, *J. Nat. Prod.*, 2006, **69**, 1231–1233.
- D. J. Cousins, in *Medicinal, essential oil, culinary herb and pesticidal plants of the labiatae*, ed. D. J. Cousins, CAB International, Wallingford, Oxford, U.K., 1994, part 2, pp. 244–284.
- D. G. Kong, H. Oh, E. J. Sohn, T. Y. Hur, K. C. Lee, K. J. Kim, T. Y. Kim and H. S. Lee, *Life Sci.*, 2004, **75**, 1801–1816.
- B. Q. Wang, *J. Med. Plants Res.*, 2010, **4**, 2813–2820.
- L. Z. Li, X. Liang, X. Sun, X. L. Qi, J. Wang, Q. C. Zhao and S. J. Song, *Org. Biomol. Chem.*, 2016, **14**, 10050–10057.
- S. Y. Lee, C. D. Y. Choi and E. R. Woo, *Arch. Pharmacol. Res.*, 2005, **28**, 909–913.
- D. W. Zhang, X. Liu, D. Xie, R. D. Chen, X. Y. Tao, J. H. Zou and J. G. Dai, *Chem. Pharm. Bull.*, 2013, **61**, 576–580.
- H. W. Luo, S. X. Chen, J. N. Lee and J. K. Snyder, *Phytochemistry*, 1988, **27**, 290–292.
- F. Asari, T. Kusumi, G. Z. Zheng, Y. Z. Cen and H. Kakisawa, *Chem. Lett.*, 1990, **19**, 1885–1888.
- W. N. He, Y. Li, Y. J. Qin, X. M. Tong, Z. J. Song, Y. Z. R. Wei, L. Li, H. Q. Dai, W. Z. Wang, H. W. Luo, X. Ye, L. X. Zhang and X. T. Liu, *Appl. Microbiol. Biotechnol.*, 2017, **101**, 6365–6374.
- A. R. Lee, W. L. Wu, W. L. Chang, H. C. Lin and M. L. King, *J. Nat. Prod.*, 1987, **50**, 157–160.
- Y. Tomita and Y. Ikeshiro, *J. Chem. Soc., Chem. Commun.*, 1987, **520**, 1311–1313.
- N. Berova, K. Nakanishi and R. W. Woody, *Circular Dichroism: Principles and Applications*, Wiley, New York, 1994, pp. 413–442.
- M. J. Don, C. C. Shen, W. J. Syu, Y. H. Ding and C. M. Sun, *Phytochemistry*, 2006, **67**, 497–503.
- Y. Y. Liu, X. Y. Liang, X. N. Yin, J. D. Lv, K. Tang, J. W. Ma, T. T. Ji, H. F. Zhang, W. Q. Dong, X. Jin, D. G. Chen, Y. C. Li, S. Y. Zhang, H. D. Q. Xie, B. Zhao, T. Zhao, J. Z. Lu, Z. W. Hu, X. T. Cao, F. X. F. Qin and B. Huang, *Nat. Commun.*, 2017, **8**, 15207.
- S. W. Huang, J. W. Qiao, X. Sun, P. Y. Gao, L. Z. Li, Q. B. Liu, B. Sun, D. L. Wu and S. J. Song, *Funct. Foods*, 2016, **24**, 183–195.

